Production of oxygen by electronically induced dissociations in ice

R. E. Johnson
Engineering Physics, Thornton Hall B103, University of Virginia, Charlottesville, VA 22904

P. D. Cooper and T. I. Quickenden
Chemistry M313, School of Biomedical and Chemical Sciences, The University of Western Australia, 35 Stirling Highway, Crawley, Western Australia 6009, Australia

G. A. Grieves
School of Chemistry and Biochemistry, Georgia Institute of Technology, Atlanta, Georgia 30332

T. M. Orlando[a)]
School of Chemistry and Biochemistry, Georgia Institute of Technology, Atlanta, Georgia 30332 and School of Physics, Georgia Institute of Technology, Atlanta, Georgia 30332

(Received 4 March 2005; accepted 9 September 2005; published online 9 November 2005)

A solid-state chemical model is given for the production of O_2 by electronic excitation of ice, a process that occurs on icy bodies in the outer solar system. Based on a review of the relevant available laboratory data, we propose that a trapped oxygen atom-water complex is the principal precursor for the formation of molecular oxygen in low-temperature ice at low fluences. Oxygen formation then occurs through direct excitation of this complex or by its reaction with a freshly produced, nonthermal O from an another excitation event. We describe a model for the latter process that includes competition with precursor destruction and the effect of sample structure. This allows us to put the ultraviolet photon, low-energy electron, and fast-ion experiments on a common footing for the first time. The formation of the trapped oxygen atom precursor is favored by the preferential loss of molecular hydrogen and is quenched by reactions with mobile H. The presence of impurity scavengers can limit the trapping of O, leading to the formation of oxygen-rich molecules in ice. Rate equations that include these reactions are given and integrated to obtain an analytic approximation for describing the experimental results on the production and loss of molecular oxygen from ice samples. In the proposed model, the loss rate varies, roughly, inversely with solid-state defect density at low temperatures, leading to a yield that increases with increasing temperature as observed. Cross sections obtained from fits of the model to laboratory data are evaluated in light of the proposed solid-state chemistry. © *2005 American Institute of Physics*.
[DOI: 10.1063/1.2107447]

I. INTRODUCTION

Oxygen has been detected in the very thin atmospheres on the icy moons of Jupiter, and peroxide and oxygen-rich molecules have been observed as trapped species in their icy surfaces. The observed O_2 is primarily a product of the decomposition of ice by energetic ions and electrons trapped in the Jovian magnetosphere.[1–4] More recently molecular oxygen ions have been detected over the rings of Saturn suggestive of an oxygen ring atmosphere produced by ultraviolet (UV) photon-induced production of O_2 in ice.[5] In addition, molecular oxygen, hydrogen peroxide, and oxidized sulfur and carbon have all been detected as trapped species *in* the icy satellite surfaces.[4,6] At the icy moon Europa, the proposed transport of these oxygen-rich species to its putative subsurface ocean as a means of sustaining aerobic life processes[7] has excited the astrophysical community. This has also motivated us to describe the solid-state chemistry that follows the production of electronic excitations in ice.

In this paper, we summarize the laboratory database for radiation-induced production of O_2 from ice. We then use these results as a guide in describing the physical and chemical processes leading to the formation of molecular oxygen by energetic charged particles (e.g., ions), electrons, and ultraviolet (UV) photons incident on an ice sample. Our goal is to characterize the primary physical and chemical pathways for the nonthermal production of oxygen in low-temperature ice. Quite remarkably, a quantitative model for this was not

radiation and simplified to obtain an approximate analytic expression for the yield of molecular oxygen from ice that can be tested experimentally. This expression also reduces to the precursor model of Sieger *et al.*[2] and Orlando and Sieger.[3] Fits of the model to the available data are used to extract primary dissociation and reaction cross sections and to show the commonality of the results for photon, electron, and fast-ion-induced chemistry. We also show that hydrogen peroxide (H_2O_2) or the superoxide (HO_2) are not necessary precursors for oxygen production from a fresh ice sample, although they likely become important at higher doses and on annealing of the irradiated samples.[8]

II. SUMMARY OF SPACE OBSERVATIONS AND LABORATORY STUDIES

Gas-phase oxygen has been observed to be associated with the icy bodies in the Jovian and Saturnian systems as discussed.[4] In addition, two well-known transitions for interacting pairs of O_2 molecules at 577.2 and 627.5 nm were observed in the reflectance spectra of Jupiter's moons Ganymede[9] and Europa.[10] These bands are associated with the O_2 dimer,[11] suggesting that molecular oxygen is locally dense, likely as an inclusion in the icy surface.[9,12] Finally, the Hartley band of O_3 has been tentatively identified in the UV absorption spectra of certain icy satellites.[13] Although the band shape suggests that additional absorbing species are present,[14] O_3 trapped within the icy surface is consistent with the presence of trapped oxygen inclusions exposed to radiation.[1,12] This feature is superimposed on a broad UV absorption extending from about 0.4 μm to shorter wavelengths and attributed to another radiolytically produced oxidant, H_2O_2, which was also identified in the infrared (IR).[15] Consistent with the above, oxygen-rich molecules appear to be produced by the radiation processing of ice containing sulfur
(SO_2 and a sulfate) and carbon (CO_2 and a carbonate).[6] Below we summarize the laboratory data bases showing a few of the principal results.

Although impurities are known to affect luminescence in ice,[16] the production of O_2 by *photolysis* was inferred via luminescence from thick samples of ice formed from purified water.[17] In most other studies, the radiation-induced production of O_2 from ice is detected in the gas phase by a quadrupole mass spectrometer (QMS) either after warming or during irradiation as an outgassed species. In the latter experiments, the production efficiency is given as a yield, the number of O_2 produced during irradiation of the sample per electron, ion, or photon incident. This is a quantity we will calculate below. In such studies, the O_2 that remains trapped in the ice is typically not measured.

Though some early radiolysis experiments were likely affected by impurities, the ion- and electron-beam results presented in this paper were carried out in ultrahigh vacuum (UHV) with very pure ice samples. Though the techniques have been described in detail, we present a brief description of the most relevant facts concerning the low-energy electron experiments.[2,3] Briefly, an UHV chamber (base pressure of 1×10^{-10} Torr) was equipped with a pulsed low-energy (5–250 eV) electron gun, a cryogenically cooled sample holder, and a QMS. The electron beam has a maximum time-averaged current density of $\sim10^{14}$ electrons/cm^2 s and a typical beam spot size of $\sim$1.5 mm. The maximum total dose used in the experiments reported here is $\sim10^{15}$ electrons/cm^2 which was achieved using pulsed irradiation over a 100 s interval. The typical pulse width was 100 μs and the frequency used was 1000 Hz. The current density per pulse never exceeded $\sim10^{10}$ electrons/cm^2 pulse. This is an effective impingement rate of one low-energy electron per 10^5 surface molecules. Even after limited phonon excitation and secondary scattering, the subsequent heating of the surface during our pulsed electron-beam dosing condition is negligible. Since there is a secondary-emission yield from ice and holes at the surface are not all neutralized by recombination,[18] measurable surface charging occurs rapidly.[19] A quasisteady state is reached at doses as low as $\sim10^{13}$ electrons/cm^2, and then the surface charge changes very slowly. Therefore, charging cannot account for the principal fluence dependence observed for the O_2 yield.

Ice thin films were grown after several freeze-pump-thaw cycles by controlled vapor deposition on either Pt(111) or graphite substrates. Note that oxygen was never observed/present in the absence of radiation. The substrates were heated resistively which allowed for temperature control from 80 to 500 K. The substrate temperature was monitored with a thermocouple and a computer-controlled feedback system drove the temperature ramp at a rate of 8 K/min. Porous amorphous solid water (PASW) samples were deposited at 80 K with a directional doser oriented approximately 70° from normal incidence. Nonporous amorphous solid water (ASW) samples were dosed between 110–120 K at normal incidence and crystalline ice (CI) samples were deposited between 150 and 155 K. Film thickness is estimated to be between 50–100 ML by comparison to published temperature-programmed desorption data.

The principal dissociation processes in ice lead to H, OH, H_2, and O, but the principal species that escape from an irradiated ice sample are those that have the lowest binding energies to ice: H_2, O_2, and H_2O. That is, surface binding and reactive pathways act as filters for the ejecta. Therefore, gas-phase O_2 coming from an irradiated sample in a vacuum can be readily detected although decomposition of bulk ice is inefficient.

At low doses the O_2 yield was found to increase linearly with dose until saturation occurs. This dependence has been seen in a number of experiments and is shown in Figs. 1(a) and 1(b) for a fast heavy ion and low-energy electrons. These yields have also been shown to be temperature dependent by a number of laboratories using several types of incident radiation. As an example, this is shown at saturation for incident 1.5 MeV Ne^+ and low-energy electrons in Figs. 2(a) and 2(b). For temperatures $<\sim140$ K, the yield of O_2 and D_2 produced from vapor-deposited ice samples at low radiation doses decreases with decreasing temperature. It has been shown repeatedly, over most of the temperature range studied, that the measured yields depend on the total dose and not the dose rate, although this has *not* been tested at the higher temperatures shown in Figs. 1 and 2. Also seen in Fig. 2(b) is a clear drop in the yield for temperatures above

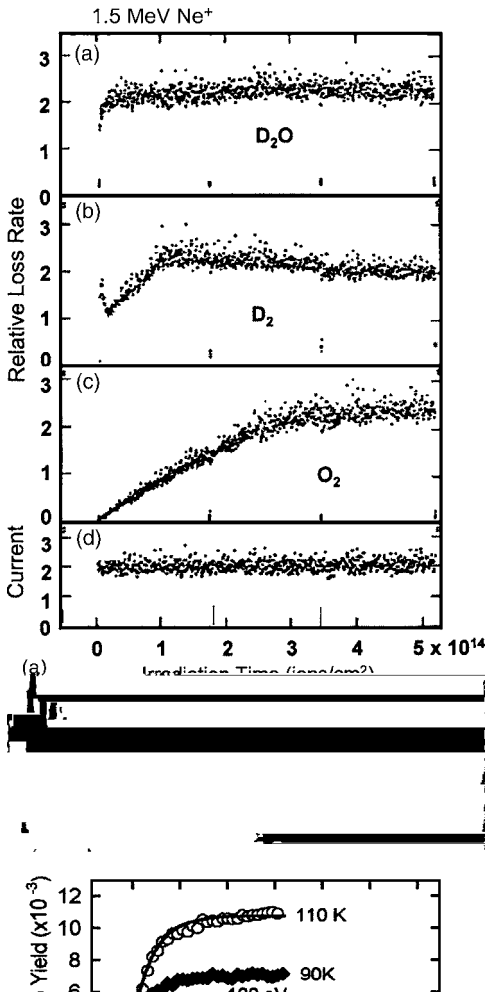

FIG. 1. (a) Relative yields vs fluence (ion flux × time) for 1.5 MeV Ne^+ incident on D_2O ice at 7 K (adapted from Reimann *et al.* 1984) (Ref. 21). Toa-25na-25nD

150 K. This drop has been shown to be related to the amorphous to cubic phase transition which is manifested by the small shoulder on the leading edge of the thermal desorption yield (solid line with no symbols) of molecular water.[3] There is also a shoulder prominent in the D_2 yield at 170 K that is due to reactive scattering in the gas phase.

The O_2 yields have also been shown to depend on the sample formation temperature and crystal state,[3] indicating that structure and defects can affect the O_2 yield. An O_2 production "threshold" of ~5.3 eV was suggested by the photolysis experiments of Mattich *et al.*[17] In the UHV experiments a threshold of ~6.5 eV (cross section $\sim 10^{-20}$ cm^2) was found using low-energy electrons[2,3] with a similar threshold for O ($^3P, ^1D$) and H_2 productions.[20] As seen in Fig. 1(a), D_2 is promptly ejected from D_2O ice whereas O_2 is not. However, after an incubation dose, the O_2 yield and D_2 yields in steady state are correlated,[21,22] as indicated in Figs. 2(a) and 2(b). In this way the stochiometry of the surface layer is only slightly altered.[23]

The temperature dependencies for the yield of O_2 from ice have been repeatedly interpreted in terms of effective activation energies. At temperatures ~40–120 K, these were found to be relatively small (~0.03 eV) [Fig. 2(a)]. Such energies are equivalent in size to activation energies for mobility of protons or hydrogen in ice and for structural rearrangements. Finally, for thin samples and penetrating radiation, percolation of oxygen from depth can occur so that the yields are found to depend on the sample thickness. Since the measured yields were also shown to depend on the excitation density, sample formation, and temperature, comparisons between experiments have proven to be difficult.

Hydrogen peroxide and related species formed by incident radiation are not readily ejected into the gas phase, but can be detected via absorption bands as trapped species in an irradiated ice sample.[24–26] Hydrogen peroxide forms via the principal dissociation product, OH, and the production yields correlate with H_2 formation.[4] Hydrogen peroxide and/or HO_2 have been suggested[2] as potential precursor species for the

formation of O_2. However, the fluence dependence observed in the QMS experiments suggests that O_2 can be formed by a process that does not involve these species, as describe below. In addition, recent matrix isolation studies indicate that trapped O can be converted to hydrogen peroxide and hydrogen peroxide converted into trapped O by incident radiation (i.e., $H_2O-O+h\nu \rightarrow H_2O_2$; $H_2O_2+h\nu \rightarrow H_2O-O$).[27] In the model below, trapped O is the principal species considered for formation of O_2 at low doses. At higher doses, the conversion of hydrogen peroxide to trapped O can provide additional channels for O_2 formation that may involve[8,28] pairs of H_2O_2 or HO_2. Although on a planetary surface the high-dose results may be more relevant, here we are primarily interested in the new channel occurring at relatively low doses in order to interpret a number of recent laboratory results. Below we construct a chemical kinetic model of the production of O_2 and then use this model to interpret a number of experiments.

III. MODEL FOR FORMATION OF O_2

The yield of O_2 from ice at low temperature increases linearly with radiation fluence (flux $\times$ time or dose) at the low fluences as indicated in Fig. 1 and is independent of beam flux. Quite remarkably, this is the case both for low-energy electrons that make a single excitation for each impact and fast ions that make a density of excitations al2-493im-T6.93i2659.9aoth2659.9thrhough2659.9thow.At is urnted of and urnted n,r The yield
rurnis-305.1os-305.1The-405.1valuhe The beam urnted of
nical that indicaring

where2

Although the density of defects, voids, and interfaces *decrease* as the formation temperature of the ice increases, the efficiency of production of O_2 is the opposite, increasing with increasing T for $T < \sim 140$ K.

We propose that trapped oxygen atoms are the principal precursor at low fluences. O_2 is then formed by the reaction of O (or OH) with this precursor or by electronic excitation of the precursor complex. Here we describe the kinetics of the production of O_2 by O-atom reactive scattering. This is similar to the production of CO_2 in a CO/H_2O ice mixture.[31] A paper describing the role of direct and indirect electronic excitations of the precursor is the subject of a separate paper.[22]

Following dissociation to H_2+O, which is given by the absorption cross section σ_d', H_2 is lost from the ice samples at the temperatures above ~40 K. The O produced by ions or electrons can be in the ground-state or in the excited singlet and triplet states. However, the UV absorption below the band gap can only produce excited singlet states. These can quench in the ice matrix releasing energy but eventually trap. The newly formed O produces an oxygen-water molecule complex, $O\cdot\cdot(H_2O)_n$, which we refer to in the following as trapped O, O_t. This occurs according to the reaction rate $k_{O,t}$, and we propose this as a precursor to the formation of O_2. This precursor might produce O_2 on excitation,[22] but here we suggest that a subsequent radiation absorption can again produce a nonthermal O via H_2+O (σ_d'). The nonthermal O can react with O_t within some reaction radius resulting in the formation of $O_2[O+O_t \rightarrow O_2]$ described by $k_{O,Ot}$. These two excitation events give a net production of two H_2 and an O_2.

The principal dissociation channel ($H_2O \rightarrow H+OH$), described by σ_d, produces a mobile H. It can also react with O_t, described by $k_{H,Ot}$, removing trapped O. Nonthermal H and O can also be removed by other reactants R [e.g., $R+H \rightarrow RH(k_{H,R}n_R)$; $R+O \rightarrow RO(k_{O,R}n_R)$, where R can be a radiation product, such as OH, or a contaminant in the ice]. Reaction of a newly formed, mobile and electronically excited OH with O_t might also produce O_2, a process that needs to be tested experimentally. We ignore this in the model and also initially ignore the conversion of trapped O to hydrogen peroxide by an electronic excitation.[4]

The principal reaction pathways considered for oxygen are

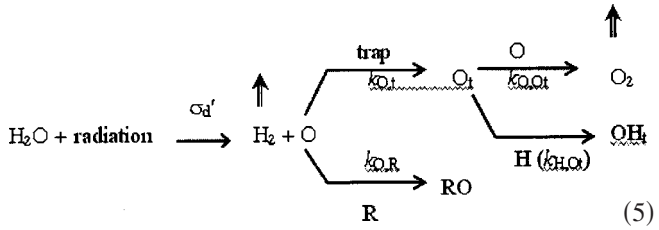

(5)

This leads to a set of rate equations:

$$dn_O/dt = \sigma_d'\phi n - k_{O,t}n_O n_t - k_{O,R}n_O n_R - k_{O,Ot}n_O n_{Ot}, \quad (6a)$$

$$dn_{Ot}/dt = k_{O,t}n_t n_O - k_{O,Ot}n_O n_{Ot} - k_{H,Ot}n_H n_{Ot}, \quad (6b)$$

$$dn_H/dt = \sigma_d\phi n - k_{H,Ot}n_H n_{Ot} - k_{H,R}n_H n_R, \quad (6c)$$

$$dn_{O_2}/dt = k_{O,Ot}n_O n_{Ot}. \quad (6d)$$

Here n_i is the density of species i in the irradiated volume and n_t is the density of trapping sites. As in Eq. (2), O_2 destruction processes are ignored in Eq. (6d), since for low-energy electrons the newly produced O_2 can escape from the excited near surface layers. For penetrating radiation this changes and O_2 that did not escape can, in principle, be dissociated by a subsequent excitation event. In addition, if direct excitation of the precursor can produce O_2, then the term $[k_{O,Ot}n_O n_{Ot}]$ in Eqs. (6a), (6b), and (6d) is replaced by a term like $\sigma_{O_2}\phi\, n_{Ot}$. The above equations act in parallel with the equations for formation of OH and hydrogen peroxide described elsewhere.[4]

Integrating the above equations over the depth of escape of O_2 from an irradiated sample, the analytic precursor model of Seiger *et al.*[2] is recovered.[4] Therefore, σ_p, σ_p', σ_{O_2} and σ can now be determined in terms of the rate constants and primary dissociation cross sections.

C. Trapped versus newly produced species

In the solid state the role of defects is critical. Defects are produced by sample formation at low-temperatures and, for penetrating radiation, defects/damage sites are produced by the irradiation itself. Since the newly produced species from an excitation event trap in times short compared to the time scale of the incident particle fluxes typically used, a steady-state background of nonthermal O does not accumulate. Therefore, the above equations can be solved simultaneously. That is, there are trapped O and freshly produced O that rapidly react or trap. If the density of traps is large, then the quantities n_H and n_t, averaged over the bombardment rate, are roughly time independent: $dn_O/dt \sim 0$ and $dn_H/dt \sim 0$. Therefore, only species trapped at defects, pores, or grain surfaces are assumed to be present before a subsequent impact. This is consistent with the lack of a dependence of the O_2 yield on the incident beam flux at those temperatures that have been tested for dose rate effects: <120 K. Solving Eqs. (6a) and (6c) for n_O and n_H, which describe the transiently mobile O and H, and substituting, Eqs. (6b) and (6d) reduce to the rate equations Eqs. (1) and (2) with O_t as the precursor.

Since the density of trapped O n_{Ot} is small compared with the density of sites at which H can react, then from Eq. (6c) $n_H \sim [\sigma_d\phi n/k_{H,R}n_R]$. For a low radiation flux ϕ, the average value of n_H is small. The O_2 yield Y_{O_2} is equal to $[(dn_{O_2}/dt)\Delta x/\phi]$ with Δx being the O_2 escape depth. The yield can now be written in the form given in Eq. (4a) with an analytic expression for the steady-state yield Y_∞,

$$[Y_\infty]/[\sigma_d' N] \approx 1 + \{(q-1) - [(q-1)^2 + 8q\delta]^{0.5}\}/4\delta,$$

$$q = [k_{O,t}(n_t + n_R)](k_{H,Ot}n_H)/(\sigma_d'\phi n)k_{O,Ot}$$
$$= (\sigma_d/\sigma_d')[k_{O,t}(n_t + n_R)]k_{H,Ot}/[k_{O,Ot}k_{H,R}n_R] \quad (7)$$

$$\delta = 0.5[1 + n_t/(n_t + n_R)].$$

We further note that for large n_t and small ϕ, q can be large. Assuming that $q \gg 1$ and that $n_t \gg n_R$, then Eq. (7) becomes

$$Y_\infty \rightarrow [\sigma_d' N]/d \approx (\sigma_d' \sigma_d' \sigma_d) N \zeta,$$
$$\zeta = [(k_{\mathrm{O,O}t} k_{\mathrm{H},R})/(k_{\mathrm{H,O}t} k_{\mathrm{O},t})][n_R/n_t] \quad (8)$$

Here the factor ζ accounts for the competing reactions. The result in Eq. (8) is based on the fact that the production of H is more efficient than the production of O (i.e., $\sigma_d \gg \sigma_d'$ so that the destruction of the precursor, O_t, by reaction with H is more efficient than the reaction with mobile O to form O_2. Comparing Eq. (8) with the expression for Y_∞ in Eq. (4b), we can write $\sigma_p \sim \sigma_d'$, $\sigma_{O_2} \sim \sigma_d'$ and $\sigma \approx \sigma_p' \sim \sigma_d$. Since mobile H and O affect both the numerator and denominator of ζ, writing $k_i \approx [\sigma_i \nu]$, where the σ_i is an interaction cross section (square of an interaction length) and ν_i the mean speed of the mobile species, the ratio $\zeta \approx [(\sigma_{\mathrm{O,O}t}\sigma_{\mathrm{H},R})/(\sigma_{\mathrm{H,O}t}\sigma_{\mathrm{O},t})] \times [n_R/n_t]$ is the ratio of interaction cross sections times the density of reaction sites to density of traps ratio. That is, the precursor destruction rate is proportional to the quenching of O_t by H, which occurs in competition with the loss of mobile H by other reactions including recombination to form H_2O. At saturation, the reaction sites are primarily dissociation products.

It is seen from Eq. (8) that the steady-state yield Y_∞ depends inversely on the density of traps n_t. That is, when the trap density is high, O_2 formation requires that a newly formed O find a trapped O before it becomes trapped or reacts with impurities or other radiation products. Therefore, the observed increase in the O_2 yield with increasing T at low doses is related to the change in the trapping density n_t with increasing temperature of the ice sample. In this model, the small activation energy measured (Fig. 2) is related to the reorientation of defects leading to a reduction in trap density. As the sample formation temperature increases and the density of traps in the bulk decreases, the surface and grain interfaces eventually become the dominant traps.[22,32] Radiation-induced defects/damage become important trapping sites for penetrating radiation and thus increases of dose can affect the production of molecular oxygen. In addition, O_2 production can increase in the presence of oxygen-rich impurities, such as CO_2 or SO_2, since their dissociation can also provide mobile O. Such species also act as hydrogen scavengers[26] affecting the destruction of O_t.

IV. COMPARISON OF MODEL TO DATA

The model above is strongly suggested by the available laboratory data on the radiolysis and photolysis of ice. Here we obtain estimates of σ_d' and σ such as those given in Table I for a few such experiments. We first consider the data for photolysis by ~10 eV photons. We then consider the parameters from the fit to the low-energy electron data and obtain parameters for the energetic ion data.

A. UV photolysis

The results of Gerakines *et al.*[25] confirm that H_2O_2 forms in ice from two OH after a buildup of trapped OH. They monitored the band associated with H_2O–HO,[33] in which the HO is bound to water with ~0.24 eV. Since they monitored a subset of the trapped OH seen in earlier experiments, additional experiments are required. Gerakines *et al.*[25] also found that peroxide production by 9.8 eV photons saturated around 10^{18} photons/cm^2. In addition, HO_2 begins to increase with fluence at about a few times 10^{17}/cm^2 shortly after they begin to detect H_2O_2. However, using Lyman-α photons (10.26 eV) Westley[34] found that O_2 formation was roughly independent of fluence down to $\sim 10^{17}$ photons/cm^2. Therefore, assuming the states accessible at 9.8 eV are similar to those excited by 10.26 eV, H_2O_2 and HO_2 exhibit a nonlinear dependence on fluence at fluences for which O_2 has reached or is approaching steady state. This comparison, in addition to the lack of a fluence offset [Eq. (5)], suggests that H_2O_2 and HO_2 are unlikely the dominant precursors at low fluences. However, experiments on the same apparatus, at the same temperature and with the same photon energy should be carried out.

TABLE I. Parameters for sample data. σ_d' is of the order of 10% of σ_d.

Radiation	E (eV)	T (K)	σ 10^{-16} cm^2	σ_d 10^{-16} cm^2	E_a (eV)
e[a]	30–100	50–120	0.8–3	~1	0.02–0.03
$h\nu$[b,c]	~10	~10	>0.1[c]	0.09[b]	0.03[c]
He^+[d]	10^6	40–140	~10		0.03
Ne^+[e]	1.5×10^6	10	62	<~35	0.02–0.07

[a]Seiger *et al.*, 1998 (Ref. 2); precursor formation $(0.5-2.0)\times10^{-18}$ cm^2 (30–100 eV) proportional to $(E-E_o)$, $E_o \sim 10$ eV, $N \sim 10^{15}$ cm^2.
[b]Watanabe *et al.*, 2000 (Ref. 29): saturation of yield of $D_2O \rightarrow 5\times10^{-19}$ cm^2.
[c]Westley *et al.*, 1995 (Ref. 34): E_{av} based on D_2O yields, σ based on lowest fluence.
[d]Brown *et al.*, 1982 (Ref. 39); based on lowest fluence.
[e]Reimann *et al.*, 1984 (Ref. 21): σ_d based on $(dE/dx)/W = 92\times10^{-15}$ eV cm^2/26 eV.

The lowest fluence studied by Westley *et al.*[34] also gives a lower limit to the precursor destruction cross section, σ. This is seen to be of the order of the Lyman-α absorption cross section in ice ($\sim 0.9\times10^{-17}$ cm^2). Using 9.8 eV photons at low T(12 K) Watanabe *et al.*[29] obtained a cross section for production of D_2 (Table I) at low fluences that is ~10–20% of the total absorption cross section with significant uncertainties. This suggests that $\sigma_d' \approx 0.1-0.2\sigma_d$ in the model above, consistent with gas-phase estimates of dissociation water molecules to O. Since photodissociation can produce an excited O, the role of the excess energy in an ice matrix needs to be evaluated.

B. Low-energy electrons

For the low-energy electron data, Sieger *et al.*[2,3] reported an O_2 production cross section of $\sim 2\times10^{-18}$ cm^2 for 100 eV incident electron energy. This is of the order of the electron impact ionization cross section for H_2O, consistent with mobile H or mobile protons as the principal destructive agents.

The O_2 yield versus fluence in these experiments was reasonably well fit by the expression in Eqs. (4). Over a narrow range of T, Sieger *et al.*[2] find $Y_\infty(T) \approx Y_\infty' \times \exp(-E_a/kT)$ with an activation energy $E_a \sim 0.02$–0.03 eV consistent with other estimates of an activation energy. Assuming that in the low-energy electron experiments

N is about 3 ML ($\sim 3\times10^{15}$ H_2O/cm^2), the measured Y_∞ gives $[\sigma_{O_2}\sigma_p/\sigma]\approx(0.5-2.0)\times10^{-18}$ cm^2 over the electron impact energy range of 30–100 eV. At 110–120 K, this ratio was found to be proportional to $E-E_o$ for $E>E_o$ ~ 10 eV, again assuming fixed N.[2,3] Using the sizes of σ and Y_∞ then one obtains $[\sigma_p\sigma_{O_2}]\sim(0.2-6)\times10^{-34}$ cm^2. This size is consistent with both σ_p and σ_{O_2} being described by events of the type $H_2O\rightarrow H_2+O(\sigma_d')$. That is, they are consistent with O being formed for $\sim$10% of the radiation-induced dissociation events ($\sigma_d'\sim0.1\sigma_d$).

The cross section for production of O may depend on the availability of dangling bonds at interfaces, in pores, or at defects, as suggested by a number of authors. However, the defect and trap densities are critical, as shown here. The role of defects is consistent with the low activation energy and differences observed in the electron-induced yield for initially crystalline and amorphous ice.[3] At relatively high T, the density of initially formed traps becomes small and the mobility of defects is high, so that the sample surface or grain interfaces are the principal trapping sites. For this reason, it is important to determine if the yield for T greater than $\sim$140 K depends on the incident flux ϕ, i.e., the dose rate. Pulsed radiolysis experiments in thick ice, in which the transients are studied rather than the steady-state yields, are required.

C. Incident ions: Escape from depth

Even though the shower of secondary electrons produced in a solid by a fast incident ion can result in multiple excitations locally, the yield versus fluence for O_2 production also varies linearly with fluence at low fluences.[21] For low T, this yield is also independent of dose rate at low-dose rates suggesting O_2 formation via a chemical precursor. The O_2 yield versus fluence in Fig. 1(a) for incident ions at low doses can also be roughly fit by the expressions in Eq. (4). However, the fit is not as good as it is for the low-energy electrons suggesting other effects are important. In addition, Y_∞ vs T was shown to have two "plateaus:" one for very low doses and one at higher doses with activation energies in the range $\sim$0.02–0.07 eV. These differences indicate that additional precursors can be formed in the ion track and that the ion penetration and escape depth for a newly produced O_2 are important. That is, the quantity N in Eq. (1) is the "depth" from which O_2 formed below the surface can percolate to the surface and escape.[35,36] Ignoring these differences and fitting the data for the incident 1.5 MeV Ne^+ at 10 K, one obtains $\sigma=60\times10^{-16}$ cm^2. This is comparable to size of the molecular destruction cross section, $\sigma_d\approx30\times10^{-16}$ cm^2 by these ions (Table I).

At saturation (steady state) a single new event leading to an O can lead to the production O_2 from the steady-state density of trapped precursors in the model proposed here. Therefore, allowing for changes in sample structure, the yield at saturation should be nearly linear in the excitation cross section. This is the case for the low-energy electrons,[2] and it was initially assumed to be the case for the fast ions.[21,37] However, Baragiola *et al.*[38] showed that for a temperature at which decomposition dominates the sputtering of ice,[39] the steady-state yield (Y_∞) is proportional to the square of the electronic energy deposition per unit path length in the solid. If the production and destruction cross sections in Y_∞ in Eq. (4b) roughly scale with $(dE/dx)_e$, the ratio $[\sigma_p\sigma_{O_2}/\sigma]$ also varies as $(dE/dx)_e$. Therefore, we propose that the quantity N in Y_∞ also varies with $(dE/dx)_e$. That is, the depth N from which O_2 can be mobilized to escape depends on the excitation density $(dE/dx)_e$. This is consistent with the observation that the O_2 yield depends on thickness for samples thinner than the ion penetration depth.[21,35] Based on the proposed model, a description of the percolation depth for escape, N, is required to compare the yields for penetrating radiation with those for nonpenetrating radiation. Since the defects/damage produced by the ions can affect both the density of traps and the percolation of O_2, the low-energy electron and UV photons experiments provide better tests of the chemistry for molecular oxygen production.

V. SUMMARY

The exciting observations of thin oxygen atmospheres and oxidants trapped in the icy surfaces on outer solar system bodies[5,6] have lead to increased interest by chemists in the radiation-induced production of oxygen in ice. Although this is a process that has been studied for a half century, quite remarkably, no quantitative model existed. In this paper we first summarized the principal results of those experiments and then give a solid-state chemical model for the production of O_2 in ice *at low doses*. The model is consistent with the available data for formation of oxygen due to electronic excitations in ice produced by fast ions, low-energy electrons, and UV photons at low temperatures.

In our model, trapped oxygen atoms are the dominant precursor to the formation of molecular oxygen at low radiation doses. The proposed rate equations are integrated to obtain an analytic model for the fluence and temperature dependences of the O_2 yield. In deriving the analytic model from the rate equations, the competition between the formation and destruction processes is accounted for. The role of trapping sites and escape from depth for penetrating radiation are also accounted for. These are both affected by the thermal and radiation histories of the sample. This has allowed us to put low-dose data for incident photons, electrons, and energetic ions on the same basis for the first time.

The proposed model suggests measurements that are needed to describe the chemical state of the irradiated ice and to interpret new laboratory data. For instance, the proposed precursor, trapped O, may be detectable. In addition, much more data are needed on the production of oxygen by UV photons, especially as this process is thought to produce the oxygen atmosphere recently observed over Saturn's rings.[5] Studies of possible dose rate affects above $\sim$140 K are needed to test the limit of applicability of the trapped precursor model. Studies of the affect of impurities, such as carbon and sulfur species, are needed as these can compete with defect sites to scavenge O. Scavenging by impurities is known to affect the radiolytic yields. This could have been a problem in the earlier experiments but, quite remarkably, more recent results, using ultrahigh vacuum and the vapor

deposition of purified water samples, give similar results. Scavenging by impurities is also of considerable astrophysical interest and has been suggested to be consistent with the observation of primarily oxygen-rich carbon and sulfur species on the icy satellites.[4,6] It has also been suggested[29] that the direct production of H_2 and the production of the precursor[2,22] will be enhanced at the ice surface or at an internal surface in a porous sample. Therefore, the correlation of the formation temperature and radiation damage with the defect density and the formation of trapped O need to be studied in detail. Finally, it is also important to describe quantitatively the relationship between H_2 loss and the competition between O_2 *and* H_2O_2 formations over a range of temperatures and fluences. Such experiments are in progress and the model above will provide a framework for interpreting new data. More importantly, this model can now be used to apply the presently available laboratory data to understanding the observations of molecular oxygen on icy bodies in the outer solar system, an exciting new aspect in planetary science.

ACKNOWLEDGMENTS

Coauthor Dr. T. I. Quickenden died on July 24, 2005. He has contributed significantly to the field dealing with radiation and photochemistry of ices and he will be missed by the community. One of the authors (R.E.J.) acknowledges support from NASA's Geology and Geophysics program and NSF's Astronomy program. Two of the authors (T.M.O. and G.A.G.) acknowledge support from NASA's Planetary Atmospheres Program No. NAG5-13234.

[1] R. E. Johnson and T. I. Quickenden, J. Geophys. Res., [Planets] **102**, 10985 (1997).
[2] M. T. Sieger, W. C. Simpson, and T. M. Orlando, Nature (London) **394**, 554 (1998).
[3] T. M. Orlando and M. T. Sieger, Surf. Sci. **528**, 1 (2003).
[4] R. E. Johnson, T. I. Quickenden, P. D. Cooper, A. J. McKinley, and C. G. Freeman, Astrobiology **3**, 823 (2003).
[5] D. A. Young, J. J. Berthelier, M. Blanc *et al.*, Science **307**, 1262 (2005).
[6] R. E. Johnson, R. W. Carlson, J. F. Cooper, C. Paranicas, M. H. Moore, and M. C. Wong, in *Jupiter: Satellites, Atmosphere and Magnetosphere*, edited by F. Bagenal (Cambridge University Press, Cambridge, UK, 2004).
[7] J. S. Kargel, J. Z. Kaye, J. W. Head III, G. M. Marion, R. Sassen, J. K. Crowley, O. P. Ballesteros, S. A. Grant, and D. L. Hogenboom, Icarus **148**, 226 (2000); C. F. Chyba and K. P. Hand, Science **292**, 2026 (2001); J. F. Cooper, R. E. Johnson, B. H. Mauk, H. B. Garrett, and N. Gehrels, Icarus **149**, 133 (2001).
[8] P. D. Cooper, R. E. Johnson, and T. I. Quickenden, Icarus **166**, 444 (2003).
[9] W. M. Calvin, R. E. Johnson, and J. R. Spencer, Geophys. Res. Lett. **23**, 673 (1996).
[10] J. R. Spencer and W. M. Calvin, Astron. J. **124**, 3400 (2002).
[11] A. U. Khan and M. Kasha, J. Am. Chem. Soc. **92**, 3293 (1970).
[12] R. E. Johnson and W. A. Jesser, Astrophys. J. **480**, L79 (1997).
[13] K. S. Noll, R. E. Johnson, A. L. Lane, D. L. Domingue, and H. A. Weaver, Science **273**, 341 (1996); K. S. Noll, T. L. Roush, D. P. Cruikshank, R. E. Johnson, and Y. J. Pendleton, Nature (London) **388**, 45 (1997).
[14] R. E. Johnson, *Chemical Dynamics in Extreme Environments*, Adv Ser Phys Chem Vol. 11 (2001), p. 390.
[15] R. W. Carlson, M. S. Anderson, R. E. Johnson *et al.*, Science **283**, 2062 (1999).
[16] G. Vierke and J. Stauff, Ber. Bunsenges. Phys. Chem. **74**, 358 (1970).
[17] A. J. Matich, M. G. Bakker, D. Lennon, T. I. Quickenden, and C. G. Freeman, J. Phys. Chem. **97**, 10539 (1993).
[18] M. T. Sieger, W. C. Simpson, and T. M. Orlando, Phys. Rev. B **56**, 4925 (1997); J. Herring-Captain, G. A. Grieves, A. Alexandrov, M. T. Sieger, H. Chen, and T. M. Orlando, *ibid.* **72**, 035431 (2005).
[19] W. C. Simpson, T. M. Orlando, L. Parenteau, K. Nagesha, and L. Sanche, J. Chem. Phys. **108**, 5027 (1998).
[20] G. A. Kimmel, T. M. Orlando, C. Vezina, and L. Sanche, J. Chem. Phys. **101**, 3282 (1994); G. A. Kimmel and T. M. Orlando, Phys. Rev. Lett. **75**, 2606 (1995); G. A. Kimmel and T. M. Orlando, Phys. Rev. Lett. **77**, 3983 (1996).
[21] C. T. Reimann, J. W. Boring, R. E. Johnson, J. W. Garrett, K. R. Farmer, W. L. Brown, K. J. Marcantonio, and W. M. Augustyniak, Surf. Sci. **147**, 227 (1984).
[22] G. A. Grieves and T. M. Orlando, Surf. Sci. **593**, 180 (2005).
[23] R. R. Rye, T. E. Madey, J. E. Houston, and P. H. Holloway, J. Chem. Phys. **69**, 1504 (1978).
[24] I. A. Taub and K. Eiben, J. Chem. Phys. **49**, 2499 (1968).
[25] P. A. Gerakines, W. A. Schutte, and P. Ehrenfreund, Astron. Astrophys. **312**, 289 (1996).
[26] M. H. Moore and R. L. Hudson, Icarus **145**, 282 (2000).
[27] L. Khriachtchev, M. Pettersson, S. Jolkkonen, S. Pehkonen, and M. Rasanen, J. Chem. Phys. **112**, 2187 (2000).
[28] P. D. Cooper, H. G. Kjaergaard, V. S. Langford, A. J. McKinley, T. I. Quickenden, and D. P. Schofield, J. Am. Chem. Soc. **125**, 6048 (2003).
[29] N. Watanabe, T. Horii, and A. Kouchi, Astrophys. J. **541**, 772 (2000).
[30] M. T. Sieger and T. M. Orlando, Surf. Sci. **390**, 92 (1997).
[31] N. Watanabe and A. Kouchi, Astrophys. J. **567**, 651 (2002).
[32] B. Rowland, M. Fisher, and J. P. Devlin, J. Chem. Phys. **95**, 1378 (1991).
[33] V. S. Langford, A. J. McKinley, and T. I. Quickenden, J. Am. Chem. Soc. **122**, 12859 (2000).
[34] M. S. Westley, R. A. Baragiola, R. E. Johnson, and G. A. Baratta, Planet. Space Sci. **43**, 1311 (1995).
[35] J. Benit and W. L. Brown, Nucl. Instrum. Methods Phys. Res. B **46**, 448 (1990).
[36] P. Ayotte, R. S. Smith, K. P. Stevenson, Z. Dohnalek, G. A. Kimmel, and B. D. Kay, J. Geophys. Res., [Planets] **106**, 33387 (2001).
[37] W. L. Brown, W. M. Augustyniak, L. J. Lanzerotti, R. E. Johnson, and R. Evatt, Phys. Rev. Lett. **45**, 1632 (1980).
[38] R. A. Baragiola, in *Water in Confining Geometries*, edited by J. P. Devlin and V. Buch (Elsevier, New York, in press).
[39] W. L. Brown, W. M. Augustyniak, E. Simmons, K. J. Marcantonio, L. J. Lanzerotti, R. E. Johnson, J. W. Boring, C. T. Reimann, G. Foti, and V. Pirronello, Nucl. Instrum. Methods Phys. Res. B **198**, 1 (1982).